REPORT DOCUMENTATION PAGE

Form Approved OMB No. 074-0188

1. AGENCY USE ONLY (Leave blank)	2. REPORT DATE	3. REPORT TYPE AND DATES COVERED
	1999	Technical Report

4. TITLE AND SUBTITLE
Sulfur Tolerance of Selective Partial Oxidation of NO to NO_2 in a Plasma

5. FUNDING NUMBERS
N/A

6. AUTHOR(S)
B.M. Pentrante, R.M. Brusasco, B.T. Merritt and G.E. Vogtlin

7. PERFORMING ORGANIZATION NAME(S) AND ADDRESS(ES)
Lawrence Livermore National Laboratory

8. PERFORMING ORGANIZATION REPORT NUMBER
N/A

9. SPONSORING / MONITORING AGENCY NAME(S) AND ADDRESS(ES)
SERDP
901 North Stuart St. Suite 303
Arlington, VA 22203

10. SPONSORING / MONITORING AGENCY REPORT NUMBER
N/A

11. SUPPLEMENTARY NOTES

12a. DISTRIBUTION / AVAILABILITY STATEMENT
Approved for public release: distribution is unlimited.

12b. DISTRIBUTION CODE
A

13. ABSTRACT ***(Maximum 200 Words)***

Several catalytic aftertreatment technologies rely on the conversion of NO to NO_2 to achieve efficient reduction of NO_x and particulates in diesel exhaust. These technologies include the use of selective catalytic reduction of NO_x with hydrocarbons, NO_x adsorption, and continuously regenerated particulate trapping. These technologies require low sulfur fuel because the catalyst component that is active in converting NO to NO_2 is also active in converting SO_2 to SO_3. The SO_3 leads to increase in particulates and/or poison active sites on the catalyst. A non-thermal plasma can be used for the selective partial oxidation of NO to NO_2 in the gas-phase under diesel engine exhaust conditions. This paper discusses how a non-thermal plasma can efficiently oxidize NO to NO_2 without oxidizing SO_2 to SO_3.

14. SUBJECT TERMS
SERDP, SERDP Collection, sulfur, NOx, particulates, diesel

15. NUMBER OF PAGES
11

16. PRICE CODE
N/A

17. SECURITY CLASSIFICATION OF REPORT	18. SECURITY CLASSIFICATION OF THIS PAGE	19. SECURITY CLASSIFICATION OF ABSTRACT	20. LIMITATION OF ABSTRACT
unclass	unclass	unclass	UL

NSN 7540-01-280-5500

Standard Form 298 (Rev. 2-89)
Prescribed by ANSI Std. Z39-18
298-102

1999-01-3687

Sulfur Tolerance of Selective Partial Oxidation of NO to NO_2 in a Plasma

B. M. Penetrante, R. M. Brusasco, B. T. Merritt and G. E. Vogtlin
Lawrence Livermore National Laboratory

ABSTRACT

Several catalytic aftertreatment technologies rely on the conversion of NO to NO_2 to achieve efficient reduction of NO_x and particulates in diesel exhaust. These technologies include the use of selective catalytic reduction of NO_x with hydrocarbons, NO_x adsorption, and continuously regenerated particulate trapping. These technologies require low sulfur fuel because the catalyst component that is active in converting NO to NO_2 is also active in converting SO_2 to SO_3. The SO_3 leads to increase in particulates and/or poison active sites on the catalyst. A non-thermal plasma can be used for the selective partial oxidation of NO to NO_2 in the gas-phase under diesel engine exhaust conditions. This paper discusses how a non-thermal plasma can efficiently oxidize NO to NO_2 without oxidizing SO_2 to SO_3.

I. INTRODUCTION

NO_2 plays an important role in several aftertreatment technologies. In selective catalytic reduction (SCR) with hydrocarbons, many studies suggest that the conversion of NO to NO_2 is an important intermediate step in the reduction of NO_x to N_2 [1-3]. On catalysts that are not very effective in catalyzing the equilibration of $NO+O_2$ and NO_2, the rate of N_2 formation is substantially higher when the input NO_x is NO_2 instead of NO. This has been observed on γ–Al_2O_3 [1], H-ZSM-5 [1], Na-ZSM–5 [4], Ce-ZSM-5 [4], ZrO_2 [5], Ga_2O_3 [5], Sn-ZSM-5 [6], In-Al_2O_3 [7], In-MFI [8] and Zn-MFI [9]. It has also been observed that Group II metal oxides in general are much more effective in the SCR of NO_2 compared to NO [10]. In lean-NO_x traps, the catalytic oxidation of NO to NO_2 on precious metals is followed by the formation of a nitrate on alkali or alkaline earth metal oxides [11-13]. In continuously regenerated particulate traps (CRT), a precious metal catalyst is used to oxidize NO to NO_2 upstream of a particulate filter; the NO_2 is then utilized to oxidize the carbon fraction of the trapped particulates [14-15].

The SCR, lean-NO_x trap and CRT technologies require low sulfur fuel because the catalyst component that is active in converting NO to NO_2 is also active in converting SO_2 to SO_3. The SO_3 leads to the formation of sulfuric acid and sulfates that increase the particulates in the exhaust and/or poison the active sites on the catalyst.

A non-thermal plasma can be used for the selective partial oxidation of NO to NO_2 in the gas-phase under lean-burn engine exhaust conditions [16]. The sulfur tolerance of several aftertreatment technologies can be substantially improved if it can be shown that a non-thermal plasma is more selective towards the oxidation of NO compared to the oxidation of SO_2.

There are several plasma chemistry problems that need to be overcome in order to achieve the selective partial oxidation of NO to NO_2 with high conversion efficiency. The first problem is the electrical energy required by the plasma. It is usually assumed that the O radical produced by the plasma is sufficient to oxidize NO to NO_2. This will require at least one O radical for every NO molecule. The electrical energy required to produce the necessary amount of O radicals would be large. The second problem is efficiency at high temperatures. At typical engine exhaust temperatures, e.g., 200°C and above, the O radical produced by the plasma can also reduce NO_2 back to NO, thus yielding a very low effective oxidation efficiency. The third problem is nitric acid production. In the presence of water vapor, the NO_2 in the plasma will quickly get converted to nitric acid. For SCR and lean-NO_x trap applications, it will be important to find a way of terminating the plasma oxidation such that NO is converted to NO_2 but not converted further to nitric acid.

This paper discusses how a non-thermal plasma can efficiently oxidize NO to NO_2 without oxidizing SO_2 to SO_3. We have performed experiments to quantify both the NO and the SO_2 oxidation in the plasma for gas mixtures containing various levels of NO, SO_2, O_2, H_2O and hydrocarbons. The experimental data are presented in Section II. Of particular interest to selective partial oxidation in the plasma is the strong coupling between the NO/SO_2 oxidation kinetics and the hydrocarbon oxidation kinetics. The experimental data have been used to validate our plasma chemistry model. The model is useful in identifying features that cannot be easily measured in the experiments. The chemical kinetics calculations are presented in Section III.

II. OXIDATION EXPERIMENTS

FTIR is the characterization method we have used to study the oxidation of SO_2. There are two possible ways to determine whether the plasma is affecting the SO_2 content. One is to examine the effluent from the processor and see if any SO_3 is formed. If it is assumed that the level of SO_3 formation is at or near zero, then the spectrometer may not be able to detect small amounts of SO_3. Furthermore, in the presence of water vapor, the SO_3 could quickly get converted to sulfuric acid; thus, the amount of SO_3 will not be indicative of the amount of SO_2 oxidation. The other method is to see if the SO_2 level is reduced beyond a point that could be attributed to statistical measurement error. This indirect SO_2 characterization method is employed in the analysis below.

A Nicolet Magna-IR 550 FTIR spectrometer equipped with a multipass White gas cell (Infrared Analysis model G-38H-NK-AU) was used to collect the FTIR spectra. The cell volume was 0.75 liter and the path length was set to four meters. The gas cell and sampling lines were heated to 120° ± 0.2°C to avoid condensation of product species and control species state and were sampled from the system directly via a diaphragm pump.

Figure 1 shows the IR spectrum for SO_2. There are two peak envelopes available for characterizing SO_2. One is located at approximately 1361 cm^{-1} (Q branch) and the other is located at approximately 1136 cm^{-1}. The 1361 cm^{-1} envelope is a fairly well developed band with PQR rotational fine structure. The chief drawback in using the 1361 cm^{-1} band is its proximity to the water bands. The 1136 cm^{-1} band is about one order of magnitude lower in absorbance compared with the 1361 cm^{-1} band, but does not suffer from the water interference.

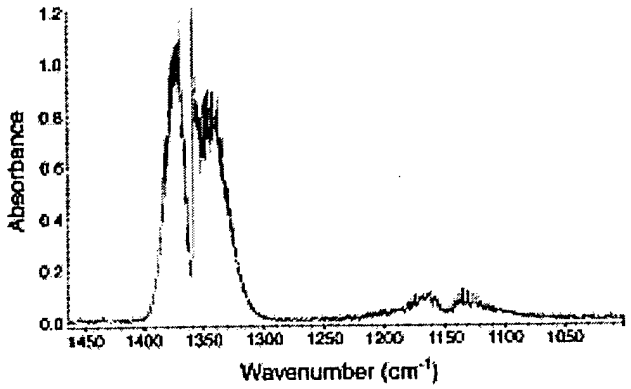

Figure 1. FTIR spectrum of SO_2 in the gas phase.

There are two possible methods to treat the 1361 cm^{-1} peak envelope in establishing changes in the SO_2 level. One is to use the Q-branch peak absorbance as the measure of the concentration of SO_2 in the gas mixture. The other is to integrate the PQR band and use the integrated peak intensity. The Q-branch method is simple to implement but suffers from more variability because of the varying population of the rotational states giving rise to the fine structure. The integrated band approach should be more repeatable since it averages out the rotational state populations. However, since this band can overlap with water peaks, it is subject to error when the water level is changing, for example, because of oxidation of hydrocarbons in the mixture; in this case we rely on the Q-branch method to establish changes in the SO_2 level.

For gas mixtures containing percent levels of water vapor, it will not be possible to use the 1361 cm^{-1} peak envelope due to strong interference from the water bands. However, with a sufficiently large amount of SO_2, the 1136 cm^{-1} envelope is available to characterize the system. There is a slight water interference in this region, but it can be shown that one can subtract out the water bands and obtain reasonable information. Therefore, the data are analyzed using the integrated intensity of the 1136 cm^{-1} band with the integration window defined as being between 1050 and 1250 cm^{-1}. The water bands are subtracted from the sample spectra using a wet syn-air blank that does not have any SO_2 present.

The 95% confidence limit in the data is determined using the standard formula,

$$95\%\ LCL = X - t(SE_m)$$

where t is the t-statistic, used because of the small sample taken (n=10) for each set of experiments. Factor X is the mean of the samples and SE_m is the standard error of the mean. To ensure that only random samples are taken and that there are no trends in the data, Figures 2 and 3 show the data collected for SO_2 in N_2 as Q-branch peak and as integrated peak absorbance, respectively.

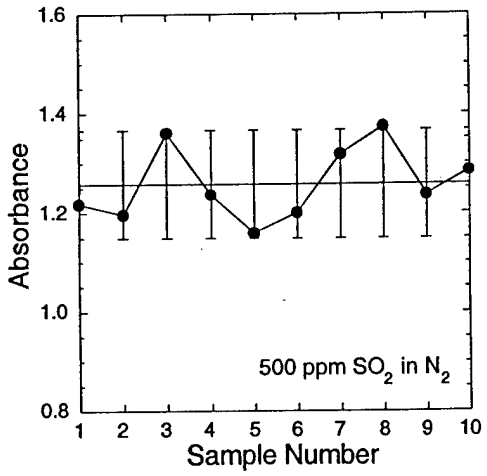

Figure 2. Absorbance of the 1361 cm^{-1} Q-branch for ten consecutive samples. The SO_2 content is 500 ppm in N_2.

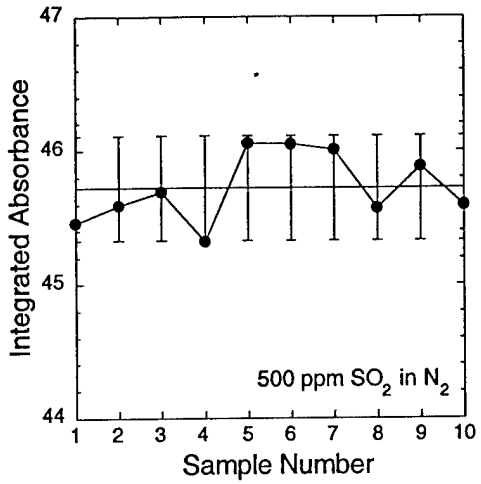

Figure 3. The 1361 cm^{-1} integrated absorbance for ten consecutive samples. The SO_2 content is 500 ppm in N_2.

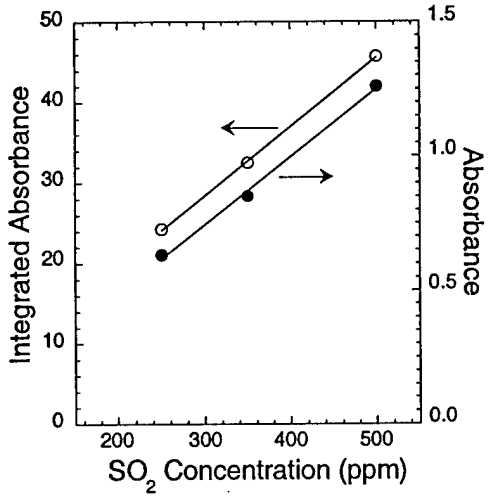

Figure 4. IR absorbance and average integrated absorbance in the 1361 cm^{-1} SO_2 peak as a function of SO_2 content.

The lack of a clear trend in the data indicates that only random sampling error is operating in these data sets. The statistical method to be used in this case is the simple application of a confidence limit applied to a mean value of the integrated IR peak absorbance reading. Since one is looking for a change in one direction only, one uses a one-tailed test and an inference is made based on one data set.

From the average values for three SO_2 concentrations, a calibration curve can be plotted to define the SO_2 content versus the IR metric, either Q-branch peak absorbance or the integrated peak intensity. These curves are shown in Figure 4; these plots are used to estimate the decrease in the SO_2 content when the plasma is applied.

The plasma reactor used in our study is a pulsed corona discharge reactor consisting of a metal wire inside a metal cylinder. The power supply is a magnetic pulse compression system that delivers up to 30 kV output into 100 ns pulses at repetition rates up to the kilohertz range. Heater bands and thermocouples are used to provide active control of the plasma processor temperature. The processor temperature can be adjusted from room temperature up to 500°C.

Although we have used a pulsed corona plasma reactor, the plasma chemistry is not peculiar to this type of plasma processor. All electrical discharge plasma reactors accomplish essentially the same gas-phase plasma chemistry under the same gas conditions [17-20].

A gas blending manifold is used to custom make gas streams consisting of N_2, O_2, H_2O, hydrocarbons, SO_2 and NO_x. These gases are metered through mass flow controllers that permitted exact control of the flow rate. After mixing in the manifold, the gas then passes through a temperature-controlled heater that preheated the gas to the processor temperature.

Six sets of experiments were done using mixtures of synthetic air in various combinations at a gas temperature of 260°C. The gas temperature chosen is typical of diesel engine exhaust temperature. The mixtures tested were:

(1) 10% O_2, 500 ppm SO_2, balance N_2

(2) 10% O_2, 500 ppm SO_2, 500 ppm NO, balance N_2

(3) 10% O_2, 500 ppm SO_2, 1000 ppm C_3H_6, balance N_2

(4) 10% O_2, 500 ppm SO_2, 500 ppm NO, 1000 ppm C_3H_6, balance N_2

(5) 10% O_2, 5% H_2O, 500 ppm SO_2, balance N_2

(6) 10% O_2, 5% H_2O, 500 ppm SO_2, 1000 ppm C_3H_6, balance N_2

These experiments use a large quantity of SO_2 and a significant plasma power level. The level of plasma power applied averaged 40 J/L, which would correspond to around 4% of the engine output power. If no oxidation effect is discovered using these reaction conditions, then it is not likely that milder conditions will present a different outcome so this can be considered a worst case scenario.

The purpose of experiment (1) is to quantify the amount of SO_2 oxidation by the O radical. Electron-impact dissociation of O_2 in the plasma produces O radicals:

$$e + O_2 \rightarrow e + O(^3P) + O(^3P, ^1D)$$

where $O(^3P)$ (simply referred to as O) and $O(^1D)$ are ground-state and metastable excited-state oxygen atoms, respectively. In the absence of water vapor, most of the $O(^1D)$ relax to the ground state O. The O radical could oxidize SO_2:

$$O + SO_2 + M \rightarrow SO_3 + M$$

where M is a third molecule such as N_2 or O_2. Ozone could also be formed:

$$O + O_2 + M \rightarrow O_3 + M$$

and the ozone could then oxidize SO_2:

$$O_3 + SO_2 \rightarrow SO_3 + O_2$$

The purpose of experiment (2) is to study the competition between the oxidation of NO and the oxidation of SO_2 by the O radical. In mixture (2) the O radicals can also be consumed in the oxidation of NO:

$$O + NO + M \rightarrow NO_2 + M$$

$$O_3 + NO \rightarrow NO_2 + O_2$$

For experiments (1) and (2) we rely on the integrated absorbance of the PQR branch. This approach is more repeatable since it averages out the rotational state populations.

Figure 5 shows the change in integrated absorbance of the PQR branch centered at 1361 cm^{-1} for gas mixtures (1) and (2), before and after exposure to a plasma. Also plotted in the figure is the 95% lower confidence limit calculated for the integrated absorbance if the drop in value after plasma application is to be considered beyond statistical chance. The 95% lower confidence limit calculation was based on the variance in SO_2 detection for a mixture of SO_2 in N_2 and is considered to be a good representation of the sensitivity of the IR instrument in the absence of water.

Based on the integrated peak area reductions observed for experiment (1), the amount of SO_2 oxidized in syn-air mixture (1) is of the order of 9 ± 2 ppm. This level of SO_2 oxidation is below the detectability of SO_3 in the spectrometer. Figure 5 also shows that the amount of oxidation of SO_2 decreased in the presence of NO. This is expected because some of the O radicals are consumed in the oxidation of NO.

The purpose of experiment (3) is to examine the competition between the oxidation of SO_2 and the oxidation of C_3H_6 by the O radical:

$$O + C_3H_6 \rightarrow \text{products}$$

The rate constants for the O + C_3H_6 reactions are much larger than that for the O + SO_2 reaction. It is therefore expected that most of the O radicals will be scavenged by C_3H_6, and the level of SO_2 oxidation will be greatly decreased.

The purpose of experiment (4) is to examine the effect of C_3H_6 on both the oxidation of NO and the oxidation of SO_2. Whereas the hydrocarbon diminishes the oxidation of SO_2, the hydrocarbon greatly enhances the oxidation of NO to NO_2. The mechanism for hydrocarbon-enhanced oxidation of NO is discussed in Section III.

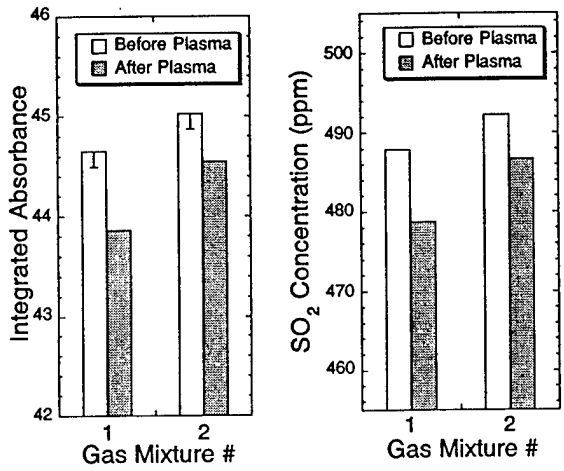

Figure 5. Change in integrated absorbance of the PQR branch centered at 1361 cm^{-1} for gas mixtures (1) and (2), before and after exposure to a plasma. The 95% lower confidence limit calculated from the "before plasma" data is indicated by the error bar.

Gas mixtures (3) and (4) contain hydrocarbon. As a result, the plasma reaction produces water vapor that interferes with the integrated peak method. The PQR band can overlap with the water peaks and therefore subject to error because of oxidation of the hydrocarbon in the mixture. We therefore rely on the Q-branch method for these experiments. The data suffers from more variability because of the varying population of the rotational states.

Figure 6 shows the change in absorbance in the 1361 cm^{-1} Q-branch peak for SO_2 for gas mixtures (3) and (4), before and after exposure to a plasma. In mixture (3), there is no detectable decrease in SO_2, as expected, because the O radicals are scavenged by the hydrocarbon. The decrease in SO_2 for mixture (4) is at the extreme edge of the confidence limit. The level of SO_2 oxidation in mixture (4) is expected to be slightly larger compared to that in mixture (3). This is because the hydrocarbon-enhanced oxidation of NO to NO_2 is accompanied by the production of OH radicals. The OH radicals could oxidize SO_2. The rate constant for the OH + SO_2 reaction is much larger compared to that for the O + SO_2 reaction. The oxidation of SO_2 by the OH radical is discussed further in the following.

Diesel engine exhaust contains 5 to 10% H_2O. In the presence of H_2O, the metastable oxygen atom, $O(^1D)$, will react with H_2O to produce OH radicals:

$$O(^1D) + H_2O \rightarrow 2\,OH$$

Additional OH radicals could be produced directly from electron-impact dissociation of H_2O:

$$e + H_2O \rightarrow e + H + OH$$

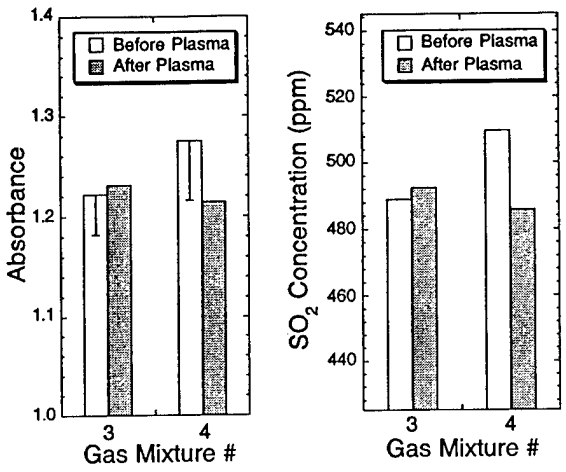

Figure 6. Change in absorbance in the 1361 cm^{-1} Q-branch peak for SO_2 for gas mixtures (3) and (4), before and after exposure to a plasma. The 95% lower confidence limit calculated from the "before plasma" data is indicated by the error bar.

The OH radical will oxidize SO_2:

$$OH + SO_2 + M \rightarrow HSO_3 + M$$

followed immediately by HSO_3 reaction with O_2 to produce SO_3:

$$HSO_3 + O_2 \rightarrow SO_3 + HO_2$$

With percent levels of H_2O, the SO_3 will quickly form sulfuric acid:

$$SO_3 + H_2O \rightarrow H_2SO_4$$

The purpose of experiment (5) is to quantify the level of SO_2 oxidation by the OH radical. This is an important experiment because it is expected that the OH radical will be responsible for any significant plasma oxidation of SO_2 in diesel engine exhaust.

The purpose of experiment (6) is to examine the competition between the oxidation of SO_2 and the oxidation of C_3H_6 by the OH radical:

$$OH + C_3H_6 \rightarrow \text{products}$$

The rate constants for the OH + C_3H_6 reactions are much larger than that for the OH + SO_2 reaction. It is therefore expected that most of the OH radicals will be scavenged by C_3H_6, and the level of SO_2 oxidation will be greatly decreased even in the presence of high levels of H_2O.

For gas mixtures (5) and (6), the presence of 5% H_2O prevents the use of the 1361 cm^{-1} peak envelope because of strong interference from the water bands. In this case we rely on the integrated intensity of the 1136 cm^{-1} band with the integration window defined as being between 1050 and 1250 cm^{-1}. The water bands are subtracted from the sample spectra using a wet syn-air blank that does not have any SO_2 present.

Figure 7 shows the change in integrated absorbance of the 1136 cm^{-1} band for gas mixtures (5) and (6), before and after exposure to a plasma. For mixture (5), the after-plasma integrated absorbance is just outside the confidence interval. The amount of SO_2 oxidized in mixture (5) is about 35 ppm.

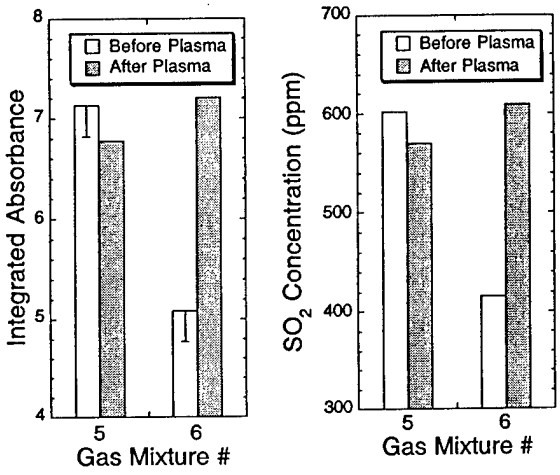

Figure 7. Change in integrated absorbance of the 1136 cm^{-1} band for gas mixtures (5) and (6), before and after exposure to a plasma. The 95% lower confidence limit calculated from the "before plasma" data is indicated by the error bar.

For mixture (6), the level of SO_2 apparently increases after the addition of plasma power. One possible explanation is the interference due to the water vapor produced by the hydrocarbon oxidation. Attempting to subtract the water spectrum due to hydrocarbon oxidation only increases the variance in the data set; the result for mixture (6) remains inconclusive. The chief difficulty in handling large amounts of water vapor stems from a diagnostic system which inadequately handles the interfering effects of water vapor. Systems can be built which more effectively deal with water vapor in the gas stream (e.g. the Perma Pure/Nafion membrane system, which we are bringing online). However, there are tradeoffs in understanding the effect of the membrane filter on the gas mixture. Although there are papers that address some of these concerns, it would still be necessary to investigate the effects of each constituent within the system and the overall performance of the system. This work is in progress.

For mixture (6), the relative increase in absorbance in the 1136 cm^{-1} integrated peak may be too much to be accounted for by water from hydrocarbon oxidation. Another possible reason for the absorbance increase in mixture (6) after addition of plasma power is the formation of formaldehyde. It is known that formaldehyde is a major

product of the partial oxidation of propene in a plasma [16]. There is no significant absorbance at 1136 cm^{-1} for formaldehyde in the gas phase. However, the hydrated form gives a broad IR peak centered at 1028 cm^{-1} with a large shoulder at 1106 cm^{-1}. It may be possible that the hydrated form of formaldehyde is produced during plasma processing of wet gas mixture (6).

To help understand what is happening in mixture (6), we rely on a chemical kinetics model that has been validated by the experimental results on mixtures (1) to (5). The difficulty in explaining the results for mixture (6) does not invalidate the results given for mixtures (1) to (5). It will be shown that the SO_2 oxidation in mixture (6) has been suppressed by the hydrocarbon. The chemical kinetics calculations are presented in the next section.

III. CHEMICAL KINETICS

Details of the plasma chemistry model used here are discussed by Penetrante et al. [16-21]. Electron-impact processes in the plasma produces ions and radicals. The efficiency for a particular electron-impact process can be expressed in terms of the G-value. The G-value is the ratio of the number of reactions to the amount of energy expended by the electrons. The G-values are calculated using the Boltzmann code ELENDIF [22], which calculates the electron energy deposition. ELENDIF uses as input the specified gas composition and the electron-molecule collision cross sections. The chemical kinetics describing the subsequent interaction of the ions and radicals with the exhaust gas is then studied using CHEMKIN-II [23]. Non-equilibrium plasma chemistry is handled by specifying G-values for forward reactions involving electron-impact dissociation and ionization of the various molecules. The chemical kinetics is determined mainly by uncharged species. In electrical discharge plasmas, the G-values for production of charged species is very small compared, for example, to that for production of O radicals. The charged species therefore do not contribute significantly to the NO_x, SO_x and hydrocarbon conversion chemistry. Most of the reaction rate constants for NO_x and SO_x are taken from compilations such as Ref. [24]. Additional hydrocarbon reaction rate constants are taken from Refs. [25-28].

Figure 8 shows the concentrations of species produced when a plasma is applied to mixture (1). The species concentrations are presented as a function of the electrical energy density in the plasma. The amount of SO_3 produced is less than 10 ppm, which is consistent with the experimental data shown in Figure 5. The most noticeable product is ozone. At high energy densities, the plasma produces NO, which is then immediately oxidized to NO_2.

Figure 9 shows the total rate (rate constant multiplied by the concentrations of reacting species) for the important reactions during plasma processing of mixture (1). Most of the O radicals are consumed in the production of ozone:

$$O + O_2 + M \rightarrow O_3 + M$$

A small amount of NO is produced by the plasma:

$$N + O_2 \rightarrow NO + O$$

The ozone is then consumed in the oxidation of NO to NO_2:

$$O_3 + NO \rightarrow NO_2 + O_2$$

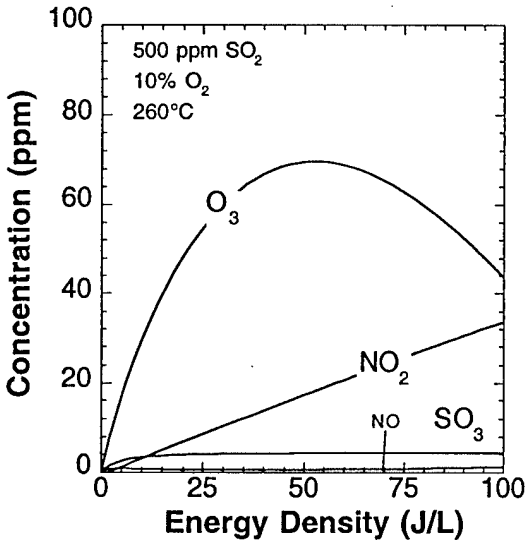

Figure 8. Calculated concentrations of species produced by plasma processing of 500 ppm SO_2 in 10% O_2, balance N_2 at 260°C.

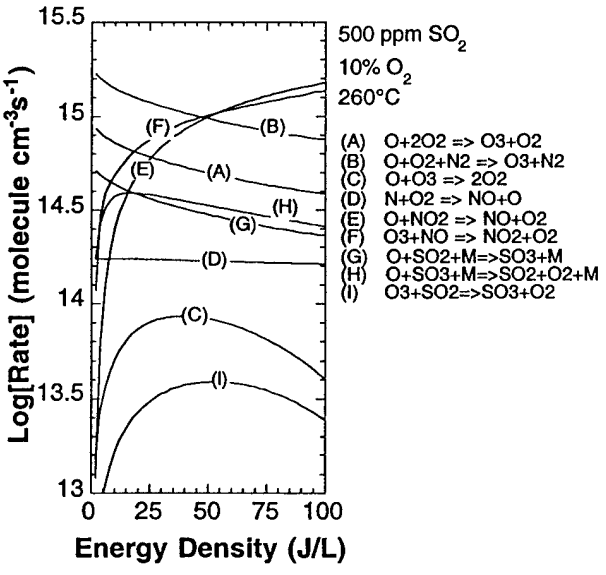

Figure 9. Analysis of the important reactions during plasma processing of 500 ppm SO_2 in 10% O_2, balance N_2 at 260°C.

The amount of SO_2 oxidation by ozone is relatively small. The SO_2 is oxidized to SO_3 directly by the O radical:

$$O + SO_2 + M \rightarrow SO_3 + M$$

The O radicals also reduce NO_2 and SO_3 back to NO and SO_2, respectively:

$$O + NO_2 \rightarrow NO + O_2$$

$$O + SO_3 + M \rightarrow SO_2 + O_2 + M$$

The backconversion of SO_3 to SO_2 accounts for the small amount of SO_3 that is formed in the plasma.

Figure 10 shows the concentrations of species produced when a plasma is applied to mixture (2). Figure 11 shows an analysis of the important reactions for mixture (2). Ozone is no longer detectable. Any ozone produced by the plasma is quickly consumed in the oxidation of NO to NO_2. A large amount of O radicals is also consumed in the oxidation of NO to NO_2. However, the efficiency for oxidation of NO to NO_2 is very low because the O radicals backconvert NO_2 to NO. Even at high energy density, the maximum oxidation of NO to NO_2 is only 10%.

SO_3 formation in mixture (2) remains low because the oxidation of SO_2 to SO_3 is counterbalanced by reduction of SO_3 to SO_2. The amount of SO_3 formed in mixture (2) is slightly less that that in mixture (1) because most of the O radicals are consumed in the oxidation-reduction reactions involving NO_x. This is consistent with the experimental result shown in Figure 5.

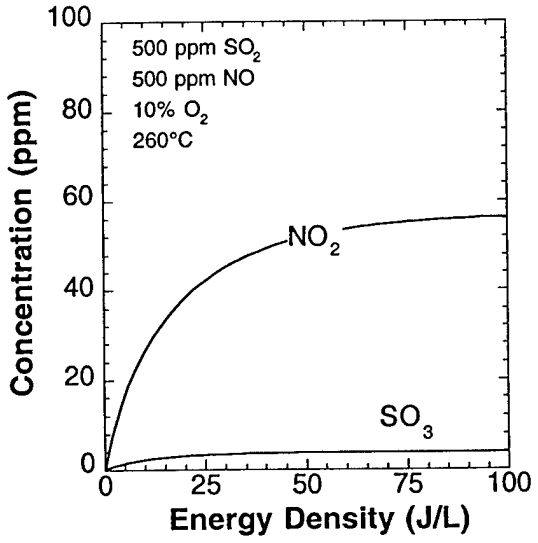

Figure 10. Calculated concentrations of species produced by plasma processing of 500 ppm SO_2, 500 ppm NO in 10% O_2, balance N_2 at 260°C.

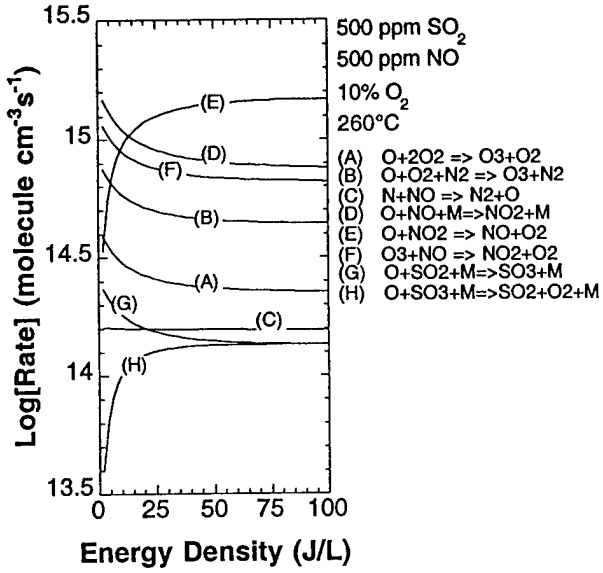

Figure 11. Analysis of the important reactions during plasma processing of 500 ppm SO_2, 500 ppm NO in 10% O_2, balance N_2 at 260°C.

Figure 12 shows the concentrations of species produced when a plasma is applied to mixture (3). Most of the O radicals are consumed in reactions with C_3H_6. SO_3 formation is very low, which is consistent with the experimental result in Figure 6.

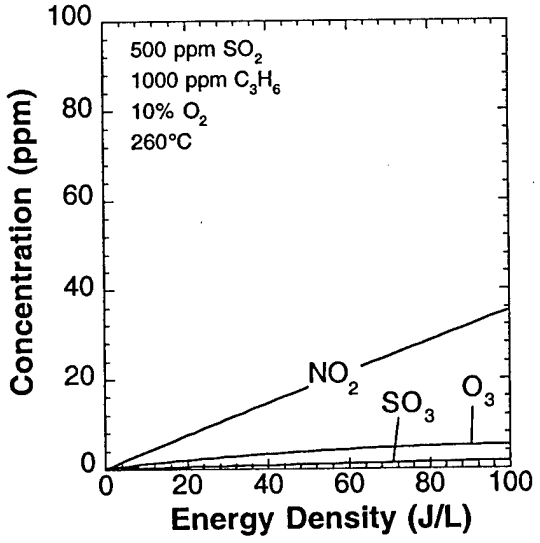

Figure 12. Calculated concentrations of species produced by plasma processing of 500 ppm SO_2, 1000 ppm C_3H_6 in 10% O_2, balance N_2 at 260°C.

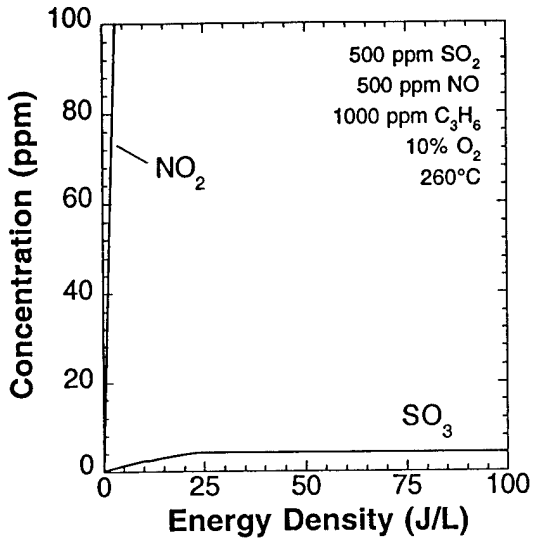

Figure 13. Calculated concentrations of species produced by plasma processing of 500 ppm SO_2, 500 ppm NO, 1000 ppm C_3H_6 in 10% O_2, balance N_2 at 260°C.

The effect of C_3H_6 on both the oxidation of NO and the oxidation of SO_2 is shown in Figure 13. The hydrocarbon greatly enhances the plasma oxidation of NO to NO_2, whereas the oxidation of SO_2 remains at a very low level. The level of SO_2 oxidation in mixture (4) is slightly larger compared to that in mixture (3), as seen in the experiment in Figure 6. This is because the hydrocarbon-enhanced oxidation of NO to NO_2 is accompanied by the production of OH radicals. The OH radicals oxidize SO_2:

$$OH + SO_2 + M \rightarrow HSO_3 + M$$

followed by HSO_3 reaction with O_2 to produce SO_3:

$$HSO_3 + O_2 \rightarrow SO_3 + HO_2$$

The amount of H_2O produced by hydrocarbon oxidation in mixture (4) is low enough so that SO_3 is not further converted to H_2SO_4.

The effect of hydrocarbons on the oxidation of NO deserves elaboration because it is the key to making the plasma process electrically efficient. At typical engine exhaust temperatures, the efficiency for conversion of NO to NO_2 is very poor in the absence of hydrocarbons in the gas stream. Figure 14 shows a comparison of our experiment to our chemical kinetics model for the case of plasma processing of 500 ppm NO in 10% O_2, balance N_2 at 300°C, without any hydrocarbon. Even with high electrical energy input, the maximum oxidation of NO to NO_2 in the plasma is only 10%. Backconversion of NO_2 to NO by the O radical is responsible for the low oxidation efficiency.

Figure 15 shows a comparison of our experiment to our chemical kinetics model for the case of plasma processing of 500 ppm NO in 10% O_2, balance N_2 at 300°C, with 1000 ppm C_3H_6. Note the dramatic increase in NO oxidation efficiency. The O radicals that normally would react with NO or NO_2 are now consumed in reactions with C_3H_6.

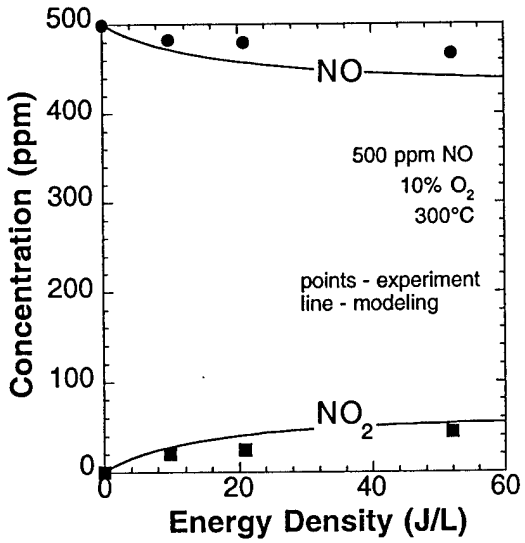

Figure 14. Plasma processing of 500 ppm NO in 10% O_2, balance N_2 at 300°C.

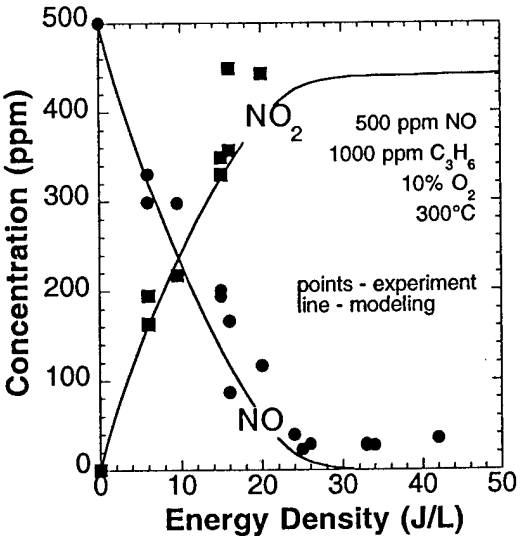

Figure 15. Plasma processing of 500 ppm NO, 1000 ppm C_3H_6 in 10% O_2, balance N_2 at 300°C.

Consider, for example, the following O + C_3H_6 reaction:

$$O + C_3H_6 \rightarrow CH_2CO + CH_3 + H$$

The H would quickly be converted to the strong oxidizing radical HO_2 upon reaction with O_2:

$$H + O_2 \rightarrow HO_2$$

and then oxidize NO:

$$HO_2 + NO \rightarrow NO_2 + OH$$

Similarly, the CH_3 will react with O_2, followed by a series of reactions that effectively oxidize NO to NO_2:

$$CH_3 + O_2 \rightarrow CH_3O_2$$

$$CH_3O_2 + NO \rightarrow NO_2 + CH_3O$$

$$CH_3O + NO \rightarrow HNO + CH_2O$$

$$HNO + O_2 \rightarrow NO_2 + OH$$

The OH radical would in turn break up more C_3H_6 molecules and lead to additional hydrocarbon radicals that could oxidize more NO to NO_2. Thus, in the presence of hydrocarbons, one O radical could initiate the oxidation of many NO molecules. Furthermore, the O radical will be prevented from backconverting NO_2 to NO.

In addition to enhancing the oxidation of NO to NO_2, the hydrocarbon is also essential in preventing the oxidation of SO_2 to sulfuric acid. Figure 16 shows the concentrations of species produced when a plasma is applied to mixture (5). In humid mixtures containing SO_2, plasma processing in the absence of hydrocarbons will produce large quantities of H_2SO_4. Figure 17 shows an analysis of the important reactions for mixture (5).

The OH radical oxidizes SO_2:

$$OH + SO_2 + M \rightarrow HSO_3 + M$$

followed immediately by HSO_3 reaction with O_2 to produce SO_3:

$$HSO_3 + O_2 \rightarrow SO_3 + HO_2$$

and then SO_3 gets converted to H_2SO_4 in the wet mixture:

$$SO_3 + H_2O \rightarrow H_2SO_4$$

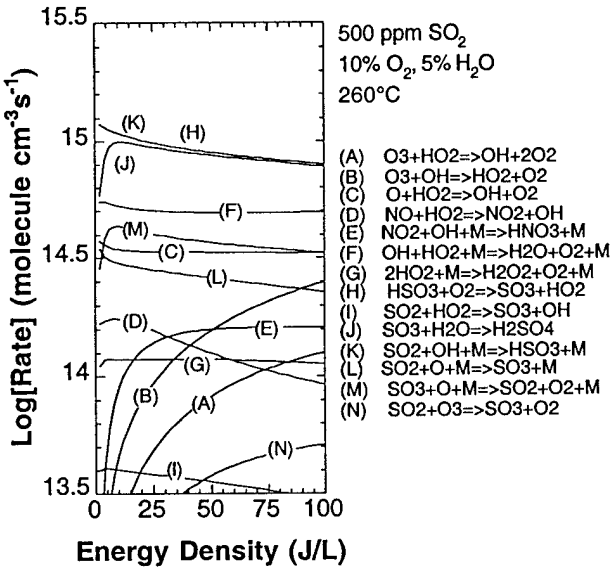

Figure 17. Analysis of the important reactions during plasma processing of 500 ppm SO_2 in 10% O_2, 5% H_2O, balance N_2 at 260°C.

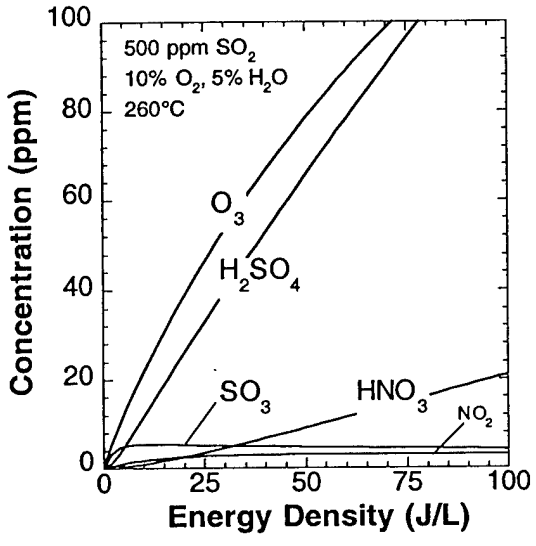

Figure 16. Calculated concentrations of species produced by plasma processing of 500 ppm SO_2 in 10% O_2, 5% H_2O, balance N_2 at 260°C.

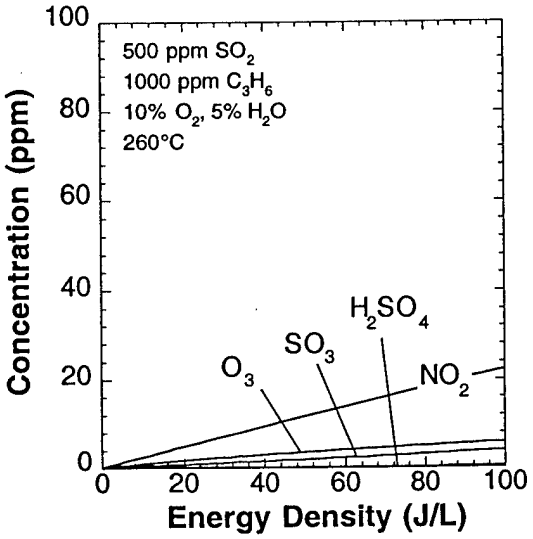

Figure 18. Calculated concentrations of species produced by plasma processing of 500 ppm SO_2, 1000 ppm C_3H_6 in 10% O_2, 5% H_2O, balance N_2 at 260°C

At an energy density of 40 J/L, the amount of H_2SO_4 formed in mixture (5) is around 50 ppm, as shown in Figure 16. This value is close to the experimentally observed SO_2 oxidation in Figure 7.

Figure 18 shows the concentrations of species produced when a plasma is applied to mixture (6). The O and OH radicals are consumed in reactions with C_3H_6. The oxidation of SO_2 is therefore suppressed.

IV. CONCLUSIONS

The use of hydrocarbons is the key to selective partial oxidation in a non-thermal plasma. The hydrocarbons play three important functions in the plasma: (1) the hydrocarbons lower the electrical energy cost for oxidation of NO to NO_2, (2) the hydrocarbons minimize the formation of acid products, and (3) the hydrocarbons suppress the oxidation of SO_2.

ACKNOWLEDGMENTS

This work was performed under the auspices of the U.S. Department of Energy under Contract Number W-7405-ENG-48, with support from the Chemical Sciences Division of the DOE Office of Basic Energy Sciences, the DOE Office of Fossil Energy, the DOE Office of Transportation Technologies, the Strategic Environmental Research and Development Program, and a Cooperative Research and Development Agreement with Cummins Engine Company. The authors thank Jordan Lampert (Engelhard Corporation, Iselin, NJ) for his critical review of the FTIR data.

REFERENCES

1. Hamada, H., Kintaichi, Y., Sasaki, M., Ito, T., and Tabata, M., "Selective Reduction of Nitrogen Monoxide with Propane over Alumina and HZSM-5 Zeolite - Effect of Oxygen and Nitrogen Dioxide Intermediate", *Appl. Catal.* **70**, L15 (1991).

2. Petunchi, J.O. and Hall, W.K., "On the Role of Nitrogen Dioxide in the Mechanism of the Selective Reduction of NO_x over Cu-ZSM-5 Zeolite", *Appl. Catal. B: Environmental* **2**, L17 (1993).

3. Shelef, M., Montreuil, C.N., and Jen, H.W., "NO_2 Formation Over Cu-ZSM-5 and the Selective Catalytic Reduction of NO", *Catal. Lett.* **26**, 277 (1994).

4. Yokoyama, C. and Misono, M., "Catalytic Reduction of Nitrogen Oxides by Propene in the Presence of Oxygen over Cerium Ion-Exchanged Zeolites: 2. Mechanistic Study of Roles of Oxygen and Doped Metals", *J.Catal.* **150**, 9 (1994).

5. Kung, M., Bethke, K., Alt, D., Yang, B. and Kung, H., in *NO_x Reduction*, ACS Symposium Series (1995).

6. Hirao, Y., Yokoyama, C., and Misono, M., "Enhancement by Water Vapour of Catalytic Reduction of NO by Propene Over Mechanically Mixed Mn_2O_3 and Sn-ZSM-5", *Chem. Comm.* March 7, 597 (1996).

7. Maunala, T., Kintaichi, Y., Inaba, M., Haneda, M., Sato, K, and Hamada, H., "Enhanced Activity of In and Ga-Supported Sol-Gel Alumina Catalysts for NO Reduction by Hydrocarbons in Lean Conditions", *Appl. Catal. B: Environmental* **15**, 291 (1998).

8. Iwamoto, M., Hernandez, A.M. and Zengyo, T., "Oxidation of NO to NO_2 on a Pt-MFI Zeolite and Subsequent Reduction of NO_x by C_2H_4 on an In-MFI Zeolite: a Novel De-NO_x Strategy in Excess Oxygen", *Chemical Communications* Jan 7 (1997) 37.

9. Iwamoto, M. and Zengyo, T., "Highly Selective Reduction of NO in Excess Oxygen through the Intermediate Addition of Reductant (IAR) Between Pt- and Zn-MFI Zeolites", *Chem. Lett.* 1283 (1997).

10. Shimokawabe, M., Ohi, A., and Takezawa, N., "Catalytic Reduction of Nitrogen Dioxide with Propene in the Presence and Absence of Oxygen Over Various Metal Oxides", *React. Kinet. Catal. Lett.* **52**, 393 (1994).

11. N. Takahashi, H. Shinjoh, T. Iijima, T. Suzuki, et al., "The New Concept 3-Way Catalyst for Automotive Lean-Burn Engine - NO_x Storage and Reduction Catalyst", *Catalysis Today* **27** (1996) 63.

12. Brogan, M.S., Brisley, R.J., Moore, J.S. and Clark, A.D., "Evaluation of NO_x Adsorber Catalyst Systems to Reduce Emissions of Lean Running Gasoline Engines", *SAE Paper* 962045 (1996).

13. Mahzoul, H., Brilhac, J.F. and Gilot, P., "Experimental and Mechanistic Study of NO_x Adsorption over NO_x Trap Catalysts", *Appl. Catal. B: Environmental*, 20, 47 (1999).

14. Cooper, B.J. and Thoss, J.E., "Role of NO in Diesel Particulate Emission Control", *SAE Paper* 890404 (1989).

15. Yoshida, K., Makino, S., Sumiya, S., Muramatsu, G. and Helferich, R., "Simultaneous Reduction of NO_x and Particulate Emission from Diesel Engine Exhaust", *SAE Paper* 892046 (1989).

16. Penetrante, B.M., Brusasco, R.M., Merritt, B.T., Pitz, W.J., Vogtlin, G.E., Kung, M.C., Kung, H.H., Wan, C.Z., and Voss, K.E., "Plasma-Assisted Catalytic Reduction of NO_x", *SAE Paper* 982508 (1998).

17. Penetrante, B.M., Hsiao, M.C., Merritt, B.T., Vogtlin, G.E., Wallman, P.H., Neiger, M., Wolf, O., Hammer, T. and Broer, S., "Pulsed Corona and Dielectric-Barrier Discharge Processing of NO in N_2", *Appl. Phys. Lett.* **68**, 3719 (1996).

18. Penetrante, B.M., Hsiao, M.C., Merritt, B.T., Vogtlin, G.E., Wallman, P.H., Kuthi A., Burkhart, C.P., and

Bayless, J.R., "Electron-Impact Dissociation of Molecular Nitrogen in Atmospheric-Pressure Non-Thermal Plasma Reactors", *Appl. Phys. Lett.* **67**, 3096 (1995).

19. Penetrante, B.M., Hsiao, M.C., Merritt, B.T., Vogtlin, G.E. and Wallman, P.H., "Comparison of Electrical Discharge Techniques for Non-Thermal Plasma Processing of NO in N_2", *IEEE Trans. Plasma Sci.* **23**, 679 (1995).

20. McLarnon, C.R. and Penetrante, B.M., "Effect of Reactor Design on the Plasma Treatment of NO_x", *SAE Paper* 982434 (1998).

21. McLarnon, C.R. and Penetrante, B.M., "Effect of Gas Composition on the NO_x Conversion Chemistry in a Plasma", *SAE Paper* 982433 (1998).

22. Morgan W. L. and Penetrante, B. M., "ELENDIF: A Time-Dependent Boltzmann Solver for Partially Ionized Plasmas", *Comp. Phys. Comm.* **58**, 127-152 (1990).

23. Kee, R. J., Rupley F. M. and Miller, J. A., "Chemkin-II: A FORTRAN Chemical Kinetics Package for the Analysis of Gas Phase Chemical Kinetics," Sandia National Laboratories Report No. SAND89-8009B UC-706 (April 1992).

24. Atkinson, R., Baulch, D.L., Cox, R.A., Hampson, Jr., R.F., Kerr, J.A. and Troe, J., "Evaluated Kinetic, Photochemical and Heterogeneous Data for Atmospheric Chemistry", *J. Phys. Chem. Ref. Data* **26**, 521 (1997).

25. Wilk, R.D., Cernansky, N.P., Pitz, W.J. and Westbrook, C.K., "Propene Oxidation at Low and Intermediate Temperatures - A Detailed Chemical Kinetic Study", *Combust. Flame* **77**, 145 (1989).

26. Koert, D.N., Pitz, W.J. and Bozzelli, J.W., "Chemical Kinetic Modeling of High Pressure Propane Oxidation and Comparison to Experimental Results", Twenty-Sixth International Symposium on Combustion, The Combustion Institute, Pittsburgh, PA, 1996, p. 633-640.

27. Pitz, W.J., Westbrook, C.K. and Leppard, W.R., "Autoignition Chemistry of C4 Olefins Under Motored Engine Conditions: A Comparison of Experimental and Modeling Results", *SAE Paper 912315* (1991).

28. Marinov, N.M., Castaldi, M.J., Melius, C.F. and Tsang, W., "Aromatic and Polycyclic Aromatic Hydrocarbon Formation in a Premixed Propane Flame", *Comb. Sci. Tech.* **28**, 295 (1997).